http://dx.doi.org/10.5012/bkcs.2012.33.8.2499

A Novel Electrochemical Method for Sensitive Detection of Melamine in Infant Formula and Milk using Ascorbic Acid as Recognition Element

Junhua Li,* Daizhi Kuang, Yonglan Feng, Fuxing Zhang, Zhifeng Xu, and Mengqin Liu

Department of Chemistry and Material Science, Hengyang Normal University, Hengyang 421008, Hunan, P. R. China
**E-mail: junhua325@yahoo.com.cn*
Received March 23, 2012, Accepted April 26, 2012

A novel and convenient electrochemical method has been developed for sensitive determination of melamine (MEL) using ascorbic acid (AA) as the recognition element. The working electrode employed in this method was modified with the nanocomposite of hydroxyapatite/carbon nanotubes to enhance the current signal of recognition element. The interaction between MEL and AA was investigated by fourier transform infrared spectroscopy and cyclic voltammetry, and the experimental results indicated that hydrogen bonding was formed between MEL and AA. Because of the existing hydrogen bonding and electrostatic interaction, the anodic peak current of AA was decreased obviously while the non-electroactive MEL added in. It illustrated that the MEL acted as an inhibitor to the oxidation of AA and the decreasing signals can be used to detect MEL. Under the optimal conditions, the decrease in anodic peak current of AA was proportional to the MEL concentrations ranging from 10 to 350 nM, with a detection limit of 1.5 nM. Finally this newly-proposed method was successfully employed to detect MEL in infant formula and milk, and good recovery was achieved.

Key Words : Electrochemical detection, Melamine, Ascorbic acid, Recognition element

Introduction

Melamine (1,3,5-triazine-2,4,6-triamine, MEL), with a chemical formula of $C_3H_6N_6$, is used primarily in the synthesis of MEL formaldehyde resins for manufacturing laminates, plastics, coatings, commercial filters, glues or adhesives, dishware, and kitchenware.[1] Because it gives analytical characteristics of protein molecules, MEL has been deliberately used by unscrupulous manufacturers to adulterate foods in order to artificially inflate the values of protein levels.[2] In fact, MEL alone has a relatively low renal toxicity. However, it is considered that MEL can bind with its co-existing impurities of triazine analogues, especially cyanuric acid, to form insoluble crystals in the kidney at very high doses, inducing acute renal failure through physical blockage of the renal tubule.[3,4] Ingestion of melamine at levels above the safety limit (2.5 ppm in the USA and EU; 1.0 ppm for infant formula milk powder in China) may cause the kidney failure and even death, especially in infants and young children.[5,6] Therefore, it is very urgent and important to develop simple, sensitive and reliable methods to detect MEL for food safety monitoring.

At present, different analytical methods, such as spectrophotometry,[7] colorimetric method,[8-12] luminescence quenching,[13] fluorescence,[14] chemiluminescence analysis,[15] surface-enhanced Raman scattering,[16] gas chromatography-mass spectrometry (GC-MS),[17] high performance liquid chromatography (HPLC),[18] sweeping micellar electrokinetic chromatography (SMEC),[19] and especially, naked eye sensing with Au nanoparticles as color indicating reporter,[20] have been reported to detect MEL with good results. However, traditional spectrophotometry and colorimetric methods are easily interfered by related compounds. Fluorescence detection can be very sensitive, but it is restricted to detect the relatively few ionic species which are native fluorescent or can be labelled with fluorescent markers, and the price of the instrument is quite high. GC-MS method can sometimes require relatively expensive reagents and need beneficiation and derivatization before analysis and it cannot be used directly to aqueous samples. HPLC and SMEC are good alternative methods, but they need high cost to buy columns and waste more organic solvents. In addition, most of these analytical methods are very time-consuming and need some special training for their operation. Thus, there is a demand for new analytical technique with cheap instrument, low cost, simple operation, time saving and real-time detection for MEL. In this regard, electrochemically analytical technique is an alternative to monitor lower concentration of MEL in food and dairy products.

Unfortunately, as a trimer of cyanamide with a 1,3,5-triazine skeleton, MEL has very good stability and relatively poor electroactivity. Even though under strong alkaline conditions, it shows a very weak electrochemical response originating from the electrooxidation of the amino group, such low sensitivity and high potential are not suitable for MEL analysis. Therefore, there are only a limited number of reports on the electroanalysis of MEL. Recently, Liao *et al*.[21] reported an electrochemical approach for MEL detection using a disposable screen printed carbon electrode with uric acid as the recognition element. It is based on the competitive adsorptive behavior of MEL at the prepared electrode causing suppression in the oxidation current of uric acid, and the decrease in peak currents can be used for MEL sensing. Liu *et al*.[22] used para-aminobenzoic acid as molecularly

imprinted polymer and hexacyanoferrate as the redox probe to develop an electrochemical sensor for the detection of MEL in milk, with a detection limit of 0.36 μM. Jin *et al.*[23] have prepared a kind of molecularly imprinted nano-porous sensing film which consisted of a graphite electrode impregnated with paraffin and modified with MEL, chitosan, silver nanoparticles and polyquercetin. This film displayed excellent and highly selective sorption of MEL and employed to detect MEL in dairy products using hexacyanoferrate as an electrochemical indicator. Liang *et al.*[24] fabricated a potentiometric sensor based on molecularly imprinted polymer for the determination of melamine in milk. Zhu *et al.*[25] also constructed a rapid, simple and sensitive electrochemical sensor for MEL based on Cu-MEL complex. In summary, these electrochemical methods were developed to detect MEL indirectly, and most of them are based on the current change of recognition element (redox probe) or adsorption of MEL on molecularly imprinted polymer. To the best of our knowledge, ascorbic acid (AA) has not yet reported as recognition element for the electrochemical determination of MEL.

In order to enhance the electrochemical response of recognition element, the working electrode employed in familiar electrochemical technique often needs surface modifying. In this paper, the working electrode was modified with multi-walled carbon nanotubes (MWCNT) and mesoporous hydroxyapatite (HAP) which were simply treated by strong acid and synthesized through preferable preparation routes, respectively. The electrochemical behaviors of recognition element were investigated in detail at modified electrodes. Compared with bare electrode and monolayer modified electrodes, the electrooxidation peak for AA was remarkably heightened at HAP/MWCNT modified electrode. However, the anodic peak current of recognition element decreased while MEL added in. It indicated that the MEL acted as an inhibitor to the oxidation of AA, and the decrease in anodic peak current can be used as an analytical signal for MEL determination. The experimental parameters such as pH value and interaction time were optimized and the interaction mechanism between MEL and AA was also discussed. Finally, this newly-proposed method was applied to detect trace amounts of MEL in infant formula and milk samples with satisfactory results.

Experimental

Reagents and Materials. MEL and AA were purchased from Sigma-Aldrich. MWCNT (purity > 95%) were obtained from Shenzhen Nanotech Port Co. Ltd. (China). The obtained MWCNT was treated by mixed acid of HNO_3/H_2SO_4 (1:3 by volume) in order to purify and segment MWCNT for easier and better dispersion, and the acid treatment caused carboxylation of MWCNT at their terminus.[26] Mesoporous HAP was successfully prepared from $Ca(NO_3)_2{\cdot}4H_2O$ and $NH_4H_2PO_4$ using surfactant cetyltrimethyl ammonium bromide as a template according to the literature.[27] A phosphate buffer solution (PBS, pH 6.0) of 0.1 M was always employed as a supporting electrolyte, and the pH value of supporting electrolyte was adjusted with 0.1 M H_3PO_4 and NaOH. All other reagents were of analytical reagent grade and used as received. All solutions were prepared with redistilled water, and the solutions were deaerated by bubbling high-purity nitrogen before the experiments.

Apparatus and Equipments. All electrochemical experiments were performed on a CHI660D electrochemical workstation (Shanghai Chenhua Co. Ltd., China) with a conventional three-electrode cell. A bare or modified glassy carbon electrode (GCE) was used as working electrode. A saturated calomel electrode (SCE) and a platinum wire were used as reference electrode and auxiliary electrode, respectively. The pH measurements were carried out on PHS-3C exact digital pH meter (Shanghai REX Instrument Factory, China), which was calibrated with standard buffer solution every day. Fourier transform infrared (FT-IR) spectra were recorded on a FTIR-8700 infrared sepectrophotometer (Shimadzu, Japan). The morphological characterizations were obtained by Tecnai G20 transmission electron microscope (TEM, FEI Corp., USA) at an accelerating voltage of 200 kV and JSM-6700F field emission scanning electron microscope (SEM, Jeol, Japan) at an acceleration voltage of 5.0 kV. All the measurements were carried out at room temperature.

Preparation of HAP/MWCNT/GCE. Before modification, a bare GCE (3 mm in diameter) was polished to form a mirror-like surface with 0.3 and 0.05 μm alumina slurry on micro-cloth pads, then washed successively with HNO_3 (1/1 by volume), anhydrous alcohol and redistilled water in an ultrasonic bath and dried in air before use. For fabrication of modified electrodes, the modifier suspension was prepared by dispersing 6.0 mg mixture of HAP and MWCNT (1/1 by mass) in 3.0 mL ethanol under ultrasonication for 30 min. This suspension of 5.0 μL was coated onto the GCE surface using a micropipette, followed by evaporating the solvent under an infrared lamp. The obtained electrode was denoted as HAP/MWCNT/GCE and the modified electrode was stored at 4 ºC in a refrigerator. For comparison, the HAP/GCE and MWCNT/GCE were fabricated with the similar procedure.

Pretreatment of Practical Samples. For analytical application, infant formula samples were pretreated according to general produce. To a centrifuge tube was added 1.0 g of dry powder and 2.0 mL water, being shaked for 1 min, and then 2.0 mL of 300 g L^{-1} trichloroacetic acid was added into. After being ultrasonically treated for 10 min, the mixture was centrifuged at 3500 rpm for 5 min to separate the deposit. The supernatant was then transferred into another centrifuge tube and adjusted to pH 6.0 with NaOH solution. The solution was centrifuged at 3500 rpm for 5 min to remove the deposit again and the final supernatant was used for detection. As far as milk sample, it was pretreated according to previous report.[8,28] Briefly, 4 mL of milk samples were mixed with 1.2 mL of 300 g L^{-1} trichloroacetic acid. After being shaked for 1 min, the mixture was centrifugated at 3500 rpm for 5 min. The supernatant was adjusted to pH

6.0 with NaOH solution before being centrifugated for another 5 min, and the final supernatant was used for detection.

Results and Discussion

Morphological Characterization of HAP/MWCNT Film. The surface morphologies of the MWCNT, HAP and HAP/MWCNT were investigated using TEM and SEM, and the obtained images are presented in Figure 1. From the TEM results, it can be seen that the diameters of all the MWCNT are in the range of 20-50 nm (Fig. 1(a)) and their average length is about several micrometers which could facilitate the establishment of a powerful network. It is also found that large quantities of well-defined HAP are obtained, and the shapes of the HAP look like irregular nanotubes with a pipe diameter of about 40-80 nm (Fig. 1(b)). However, the average length of all the HAP is about 100 nm; the small particle size can increase the specific surface area for the film and is beneficial to form porous structure. From the whole view of TEM (Fig. 1(c)) and SEM (Fig. 1(d)) images, the HAP nanotubes are well-distributed and surrounded by a lot of MWCNT, and they are interlocked together to form netlike and highly mesoporous nanostructure. So, the HAP/MWCNT film possesses rough surface and three-dimensional network structure, and the pore diameter is approximately 40 nm. This structure could provide an increase of effective surface area for superior substance adsorption and effective substrate diffusion, which is an important issue for improving the response properties of the electrochemical sensors.

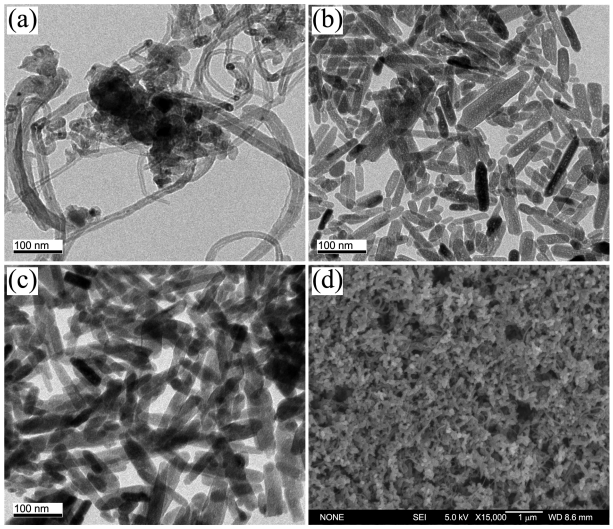

Figure 1. TEM images of (a) MWCNT, (b) HAP and (c) HAP/MWCNT films; SEM image of (d) HAP/MWCNT film.

FT-IR Spectroscopy. To investigate the interaction between AA and MEL, FT-IR spectroscopy was performed and the results are listed in Figure 2. A mixture of MEL and AA in 1:2 mole ratios was prepared to make the MEL-AA complex. From the FT-IR spectra, the 3000-3500cm^{-1} peaks (curve a) correspond to -NH_2 symmetrical and asymmetrical stretching for MEL, and 3050-3600 cm^{-1} peaks (curve b) correspond to -OH stretching vibrations for AA. However, these vibrations were completely broadened in the complex of MEL-AA (curve c), and the broadened peak between 3200-3550 cm^{-1} represents the associating peak of hydrogen bonding. It can be concluded that the vibrations of -NH_2 and -OH groups have been weakened and the hydrogen bonding has been formed in the complex. On the other hand, the peaks at 1755 cm^{-1} for C=O stretching vibration, 1320 cm^{-1} for C-O-C asymmetrical stretching and 1026 cm^{-1} for C-O-C symmetrical stretching didn't shift, so it is evident that the hydrogen bonding couldn't generate by utilizing the oxygen atom from C=O and C-O-C groups of AA. Therefore, the H-bonding (O-H···N and N-H···O) between the -OH group of

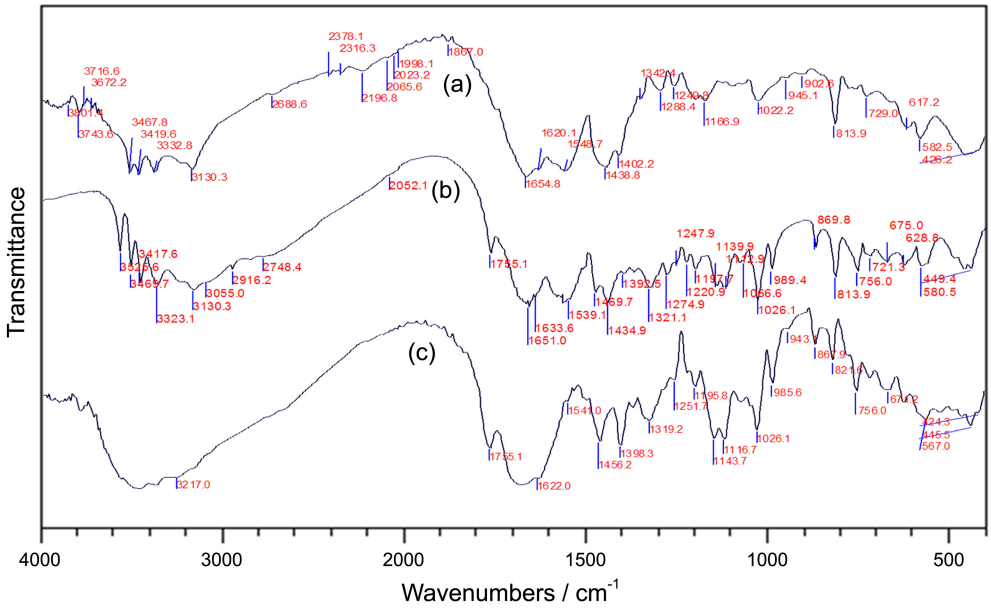

Figure 2. FT-IR spectra of (a) MEL, (b) AA and (c) MEL-AA complex.

AA and the -NH_2 of MEL is responsible for the formation of the MEL-AA complex. To our knowledge, the hydrogen bonding interaction between MEL-AA is due to the MEL molecular structure. The nitrogen atom in amino of MEL has four orbital directions which contain a double electronic rail, an atomic orbital, and two molecular orbits formed with hydrogen atoms. The hydrogen atoms in the molecular orbits are in the "half-naked" condition, and they can easily slide out from the side of the molecular orbit by the motion of the organism. After that, the nitrogen atoms from MEL can strongly attract hydrogen atoms of AA to form a new orbit, resulting in hydrogen bonding appearance between MEL-AA. Since the excessive amino and hydroxyl in the complex, the formed hydrogen bonding may be adequate and strong. Moreover, the configuration of complex is relatively stable due to the plane structure of MEL. Finally, the peaks between 1500 to 500 cm^{-1} in the three curves have analogous shapes which are mostly regarding as single bone characteristic vibrations, such as C-H swing and C-C skeletal vibration. Therefore, the FT-IR spectroscopy results have proved that the hydrogen bonding interaction exist between MEL and AA.

Electrochemical Behaviors of AA. Figure 3(A) showed cyclic voltammetry (CV) results of 0.5 μM AA at GCE (a), HAP/GCE (b), MWCNT/GCE (c) and HAP/MWCNT/GCE (d) in 0.1 M PBS (pH 6.0). There were well-defined oxidation peaks observed during the sweep from –1.0 to 1.0 V at the electrodes. However, no corresponding reduction peaks were observed. It suggests that the electrode response of AA is a typical of totally irreversible electrode reaction, which is in accordance with other reports.[29-31] Compared with GCE and monolayer modified GCE, the oxidation current at HAP/MWCNT/GCE greatly increased and the oxidation potential shifted more negatively, which might be attributed to the synergetic catalytic activity of MWCNT and HAP. In other words, the negative potential shift indicates the significant electrocatalytic activity of the modified electrode, and the current increase could be attributed mainly to a surface accumulation ability of the nanocomposite resulting from the highly mesoporous nanostructure. The extraordinarily electrocatalytic activity of this nanocomposite can give a strong analytical signal for AA, so AA could be used as a recognition element to detect non-electroactive MEL in this work. Furthermore, the influence of nanocomposite ingredient on electrochemical response of AA was also investigated by CV. Taking the mass ratio of HAP-MWCNT as 1/3, 1/2, 1/1, 2/1 and 3/1, the maximum oxidation current of AA was obtained at HAP/MWCNT film with mass ratio of 1/1.

Figure 3(B) shows the CVs of HAP/MWCNT/GCE at

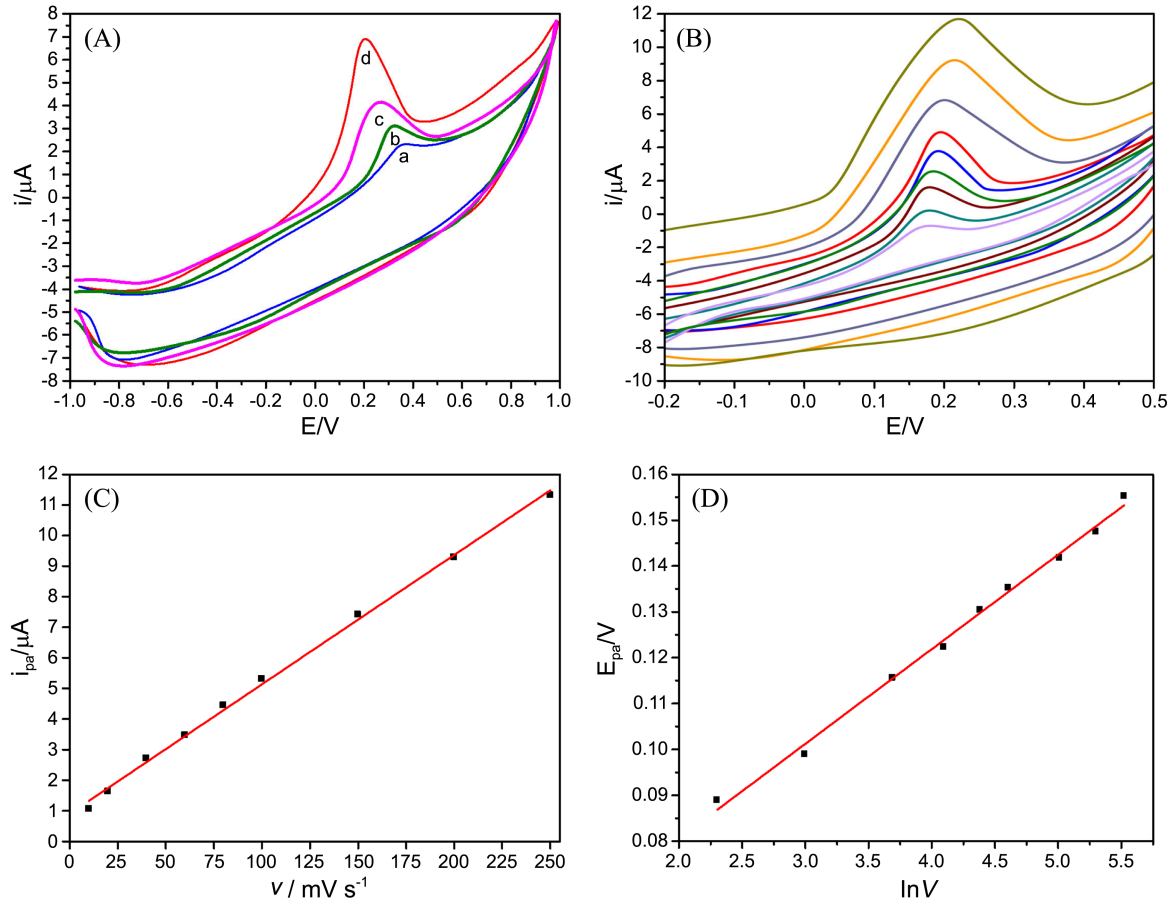

Figure 3. (A) CVs of 0.5 μM AA at GCE (a), HAP/GCE (b), MWCNT/GCE (c) and HAP/MWCNT/GCE (d) in 0.1 M PBS (pH 6.0); (B) CVs of 0.5 μM AA at HAP/MWCNT/GCE with different scan rates (10-250 mV s^{-1}) in 0.1 M PBS (pH 6.0); (C) The plot for the dependence of peak current on the scan rate; (D) The relationship between E_{pa} and ln*v*.

various scan rates from 10 to 250 mV s^{-1} obtained in 0.1 M PBS (pH 6.0) containing 0.5 μM AA. As seen from the Figure 3(C), the anodic peak current increased linearly with the scan rate in the range of 10-250 mV s^{-1} and it can be expressed as: I_{pa} (μA) = 0.04232 v (mV s^{-1}) + 0.90173 (R^2 = 0.9975). The results demonstrate that the oxidation of AA on HAP/MWCNT/GCE is a typical adsorption-controlled process. In addition, with increasing scan rate, the anodic peak potential (E_{pa}) shifted positively. The relationship between E_{pa} and the natural logarithm of scan rate (ln$v$) was shown in Figure 3(D). It can be seen that E_{pa} changed linearly versus ln$v$ with a linear regression equation of E_{pa} (V) = 0.0206 ln$v$ + 0.0393 (v, mV s^{-1}, R^2 = 0.9944) in the range from 10 to 250 mV s^{-1}. For a totally irreversible electrode process, the relationship between the potential (E_p) and scan rate (v) could be expressed as Eq. (1) given by Laviron: [32]

$$E_{pa} = E^0 + \left(\frac{RT}{\alpha nF}\right)\ln\left(\frac{RTk^0}{\alpha nF}\right) + \left(\frac{RT}{\alpha nF}\right)\ln v \qquad (1)$$

Where α is the electron transfer coefficient, n is the number of transferred electrons, R, T and F have their usual meanings. Thus, αn was calculated to be 1.21. Generally, α is assumed to be 0.5 in a totally irreversible electrode process. Finally, the number of transferred electrons (n) in the electrooxidation of AA is calculated to be 2, and the obtained transferred electron number in this work is equal to that from L-cysteine modified electrode.[33]

Electrochemical Behaviors of MEL-AA Complex. In order to make clear the electrochemical behaviors of MEL-AA complex, the CV was firstly employed to investigate the electrochemical behaviors of AA and MEL-AA at HAP/MWCNT/GCE, respectively. In blank electrolyte of PBS (pH 6.0), the redox peaks didn't appear at HAP/MWCNT/GCE in Figure 4(B) (curve a), indicating the HAP/MWCNT composite film itself was non-electroactive in the selected potential region. When 0.5 μM AA was added in the blank electrolyte, a well-define oxidation peak of AA was observed with a high anodic current (curve b). However, a significant decline (2.086 μA) in anodic current was achieved while 0.1 μM MEL was added into the above solution (curve c). In addition, Figure 4(A) shows the typical CVs of 0.5 μM AA (a) and 0.1 μM MEL (b) in 0.1 M PB (pH 6.0), respectively. There is an excellent oxidation peak for AA, but no redox peaks was observed for MEL. It suggests that HAP/MWCNT is an effective mediator in the electrocatalytic oxidation of AA, and MEL is hard to be oxidized in the selected potential region because its molecular structure is very stable. Thus, the presence of MEL induced an obvious decrease of anodic peak currents of AA at HAP/MWCNT/GCE. The decrease in the current signal of AA is attributed to the strong interaction between MEL and AA. The hydroxyl groups of AA can bind to MEL through hydrogen-bonding to form a non-electroactive complex (shown in Fig. 6), and the hydrogen-bonding also restricts the oxidation ability of the hydroxyl groups in the lactone ring, which eventually leads to a decrease in the peak currents of AA. Moreover, the carboxyl groups at the MWCNT also provoke the adsorption of MEL,

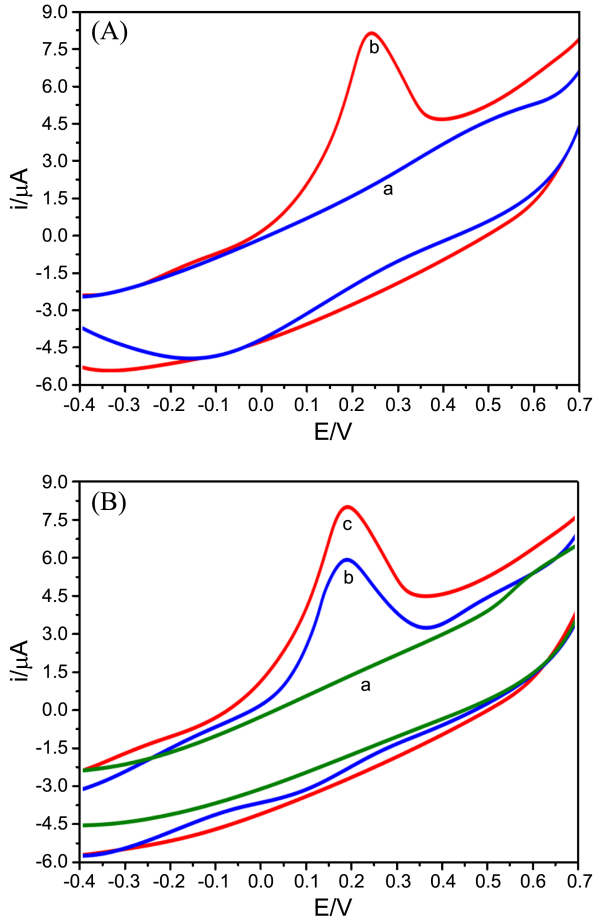

Figure 4. (A) CVs of 0.1 μM MEL (a) and 0.5 μM AA (b) at HAP/MWCNT/GCE in 0.1 M PBS (pH 6.0), respectively; (B) CVs of blank solution (a), AA (b), and MEL-AA (c) at HAP/MWCNT/GCE in 0.1 M PBS (pH 6.0).

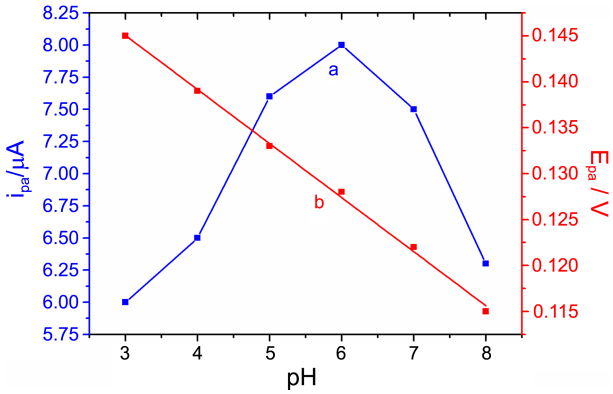

Figure 5. Effect of pH on the oxidation current (a) and oxidation potential (b) of AA at HAP/MWCNT/GCE in 0.1 M PBS.

which noticeably reduced the active sites where AA reacted (Described later in detail). Therefore, the decrease in anodic current of AA can be used as an analytical sign to detect MEL.

The pH Effect. The effect of pH on the oxidation of 0.5 μM AA at HAP/MWCNT/GCE was investigated by CV in the pH range from 3.0 to 8.0. As shown in Figure 5(a), the

anodic peak current of AA increased gradually with increasing pH from 3.0 to 6.0, and the maximum current was achieved at pH 6.0. With further increasing pH, the anodic peak current conversely decreased. Therefore, pH 6.0 was chosen for the subsequent analytical experiments. With the solution pH increasing from 3.0 to 8.0, the E_{pa} of AA at HAP/MWCNT/GCE shifted negatively and linearly (Fig. 5(b)), demonstrating that protons take part in their electrode reactions. The linear regression equation can be expressed as E_{pa} (V) = –0.0589 pH + 0.1627 (R^2 = 0.9977). The slope is approximately close to the theoretical value of −57.6 mV pH^{-1}, indicating that the electron transfer was accompanied by an equal number of protons in electrode reaction.[34] Because the number of transferred electron have been calculated to be 2 in above text, the electrooxidation of AA on HAP/MWCNT/GCE can be explained by a two-electron and two-proton mechanism (shown in Fig. 6), which is in good agreement with the previous reports.[31,35,36]

Effect of Interaction Time. The interaction degree between MEL and AA depends on the interaction time. We examined the reaction between 0.1 μM MEL and 0.5 μM AA by monitoring the CVs of the mixture at different intervals at room temperature. The anodic peak currents of AA exhibited a maximum decrease within 9 min and reached a constant value over the next 9 min, revealing that the reaction between MEL and AA is almost complete within 9 min in this work. Therefore, 9 min was chosen as the reaction time to detect MEL.

Effect of Effective Surface Area (A) and Surface Coverage (Γ_s). Since the electrode reaction of AA is controlled by the adsorption process, the surface coverage could affect the oxidation reaction. In order to demonstrate the fact that the decrease of peak currents of AA is due to the smaller adsorption of the AA while MEL added in rather than the increasing viscosity of the solution, a chronocoulometry experiment was designed in 0.5 mM $K_3[Fe(CN)_6]$ solution to get the electrochemical effective surface area for modified GCE firstly by the slope of the plot of Q *vs.* $t^{1/2}$ based on the following equation given by Anson:[37]

$$Q(t) = \frac{2nFAcD^{1/2}t^{1/2}}{\pi^{1/2}} + Q_{dl} + Q_{ads} \quad (2)$$

where A is effective surface area of working electrode, c is concentration of substrate, n is the number of transferred electron (n of $K_3[Fe(CN)_6]$ is 1), D is diffusion coefficient (D of $[Fe(CN)_6]^{3-}$ is 7.6×10^{-6} cm^2 s^{-1}),[38] Q_{dl} is double layer charge which could be eliminated by background subtraction, Q_{ads} is Faradaic charge. Other symbols have their usual meanings. Based on the slope of the linear relationship between Q and $t^{1/2}$, the effective surface area A could be calculated to be 0.0791 cm^2 and 0.147 cm^2 for GCE and HAP/MWCNT/GCE, respectively. The results indicated that the electrode effective surface area was increased obviously after electrode modification, which would increase the adsorption capacity of AA, and then lead to enhance current response for the prepared electrochemical sensor. The Faradic charge (Q_{ads}) of AA and MEL-AA mixture at HAP/MWCNT/GCE can also be measured using chronocoulometry based on equation (2). After background subtraction, the plot of Q against $t^{1/2}$ showed a linear relationship with slope of 4.23×10^{-4} C $s^{-1/2}$ and Q_{ads} of 1.20×10^{-5} C for AA, with slope of 4.45×10^{-4} C $s^{-1/2}$ and Q_{ads} of 0.579×10^{-5} C for MEL-AA mixture. As n = 2, A = 0.147 cm^2 and c = 0.1 mM, D was calculated to be 1.74×10^{-8} cm^2 s^{-1} and 1.93×10^{-8} cm^2 s^{-1} for AA and MEL-AA mixture, respectively. According to the equation of $Q_{ads} = nFA\Gamma_s$, the adsorption capacity of Γ_s could be obtained as 4.21×10^{-8} mol cm^{-2} for AA which is much higher than that for MEL-AA mixture (2.04×10^{-8} mol cm^{-2}); and the obtained Γ_s is also higher than the coverage of mono-molecular layer, so it further demonstrates that HAP/MWCNT/GCE has excellent adsorption property towards AA. It also indicates that the adsorption of AA decreases along with the MEL increase.

Since the pK_a of MEL is 8.0,[39] the amino groups of MEL could be protonated in pH 6.0 PBS solution. Moreover, carboxyl with negative charge has been grafted in the surface of MWCNT during the acid-treated process. Thus, protonated MEL can also interact with the negatively charged

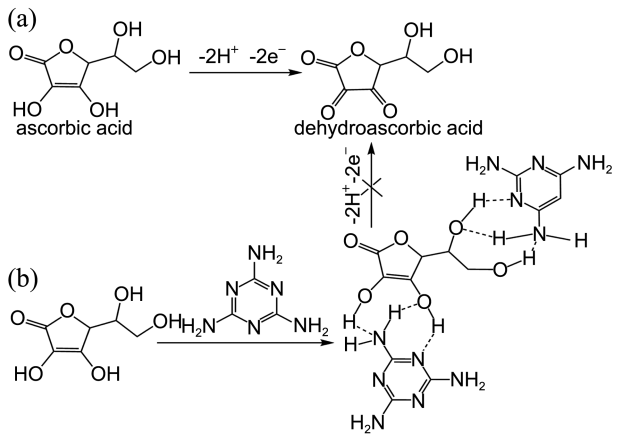

Figure 6. (a) The oxidation process of AA; (b) Hydrogen-bonding formed between MEL and AA.

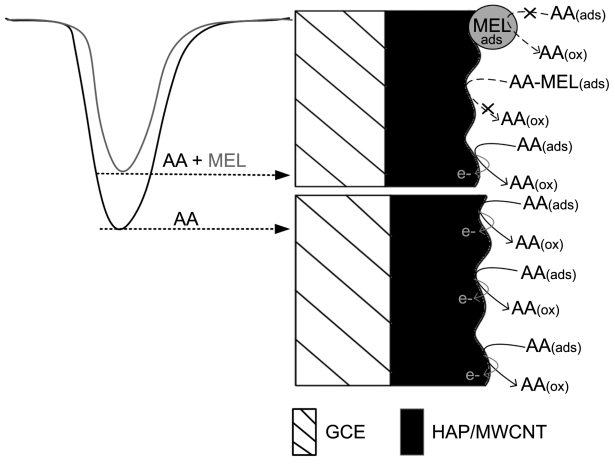

Figure 7. Schematic diagram of the detection mechanism of the proposed method.

MWCNT/HAP film through electrostatic attraction. This suggests that the presence of MEL gives rise to suppress the absorption of AA at the HAP/MWCNT/GCE, and it can be regarded as an inhibitor for oxidation of AA. Therefore, when the HAP/MWCNT/GCE was immersed in the solution containing MEL, the cavities in the film were partially occupied by MEL, which led to the decrease of the coverage and current signal of AA (seen in Fig. 7). Form the above statement, we know that the higher the concentration of MEL was, the lower the current would be. Therefore, we presume that the decrease in anodic current of AA was not only due to the hydrogen-bonding interaction between MEL and AA but also the electrostatic interaction between MEL and nanocomposite.

Electrochemical Determination of Melamine. In this study, differential pulse voltammetry (DPV) was employed for the quantitative determination of MEL, which is relatively sensitive compared to the conventional CV method. Figure 8 shows the DPV responses of various concentration of MEL in 0.1 M PBS (pH 6.0) with a constant amount of 0.5 μM AA as the recognition element. Under the optimized experimental conditions, the decrease of anodic peak current of AA was proportional to MEL concentration in the range of 10-350 nM. The linear regression equation can be expressed as ΔI_{pa} ($\Delta I_{pa} = I_{pa}$ of AA I_{pa} of MEL-AA, μA) = 0.0115C (nM) + 0.1009, with a correlation coefficient of 0.9942. The limit of detection was 1.5 nM, which was calculated according to the International Union of Pure and Applied Chemistry (IUPAC) definition that is 3 times the standard deviation of the blank value. To further investigate the performance of this proposed sensor, we have compared the results obtained above with other methods (listed in Table 1). From the Table, we know that the prepared electrochemical sensor exhibits remarkable advantages, such as the high sensitivity, a wide linear range and the low detection limit. It is noticed that the recovery obtained in this method meets the requirements for determining MEL in real samples. Therefore, the proposed method is suitable for simple-operation, low-cost and real-time analysis of MEL.

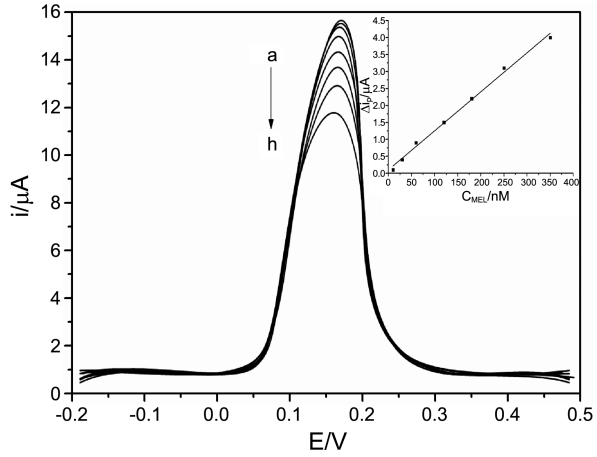

Figure 8. DPV curves of increasing MEL concentration in 0.1 M PBS (pH 6.0) containing 0.5 μM AA, from a→h, MEL of 10, 30, 60, 120, 180, 250, 350 nM, respectively. Insert: the dependence of decrease of peak currents of AA on the concentrations of MEL. Amplitude: 0.05 V; pulse width: 0.05 s; pulse period: 0.2 s; waiting time: 9 min.

Repeatability, Stability and Interference. The fabrication reproducibility for ten sensors was carried out by comparing the decrease in anodic current of 0.5 μM AA while 0.1 μM MEL added in. The relative standard deviation (RSD) was 3.25%, revealing that the proposed method had good repeatability. The stability of the electrode was also investigated by measuring the electrode response with 0.5 μM AA. After the electrode was exposed to air for 30 days at room temperature and used at least 60 times, it retained 88.6% of its original response, suggesting acceptable storage stability. On the other hand, in order to evaluate the selectivity of the electrochemical sensor, the influences of some interfering

Table 1. Comparison of the prepared sensor for MEL detection with other methods

Methods	Linear range (nM)	Detection limit (nM)	Recovery (%)	RSD (%)	Analytical samples	Refs.
Colorimetric detection	4.8-1600	0.64	93-107	–	Liquid milk	[9]
Luminescence quenching method	3-1000	0.33	98.88-101.3	2.42-4.38	Milk samples	[10]
Fluorometric detection	0.8-80	0.61	97.92-98.54	–	Milk power	[11]
Chemiluminescence analysis	0.2-80 (μg mL^{-1})	0.12 (μg mL^{-1})	86.1-102.1	0.51-1.72	Milk products	[12]
gas chromatography-mass spectrometry method	10-750 (mg kg^{-1})	2.38 (mg kg^{-1})	96.437-100.887	5.53-7.74	Animal feed	[14]
High-performance liquid chromatography	0.1-50 (μg mL^{-1})	18 (μg kg^{-1})	85.5-99.3	2.3-3.7	Liquid milk	[15]
Electrochemical detection (uric acid as recognition element)	0-126 (ppb)	1.63 (ppb)	98.17-99.20	1.32	Milk samples	[17]
molecularly imprinted polymer method	4000-450000	360	95.6-105.2	≤ 3.8	Milk samples	[18]
Electrochemical detection (oligonucleotides modified electrode)	39-3300	9.6	95	–	Liquid milk	[39]
Chemiluminescent enzyme immunoassay	62.5-2000 (ppb)	1.12 (ppb)	31.91-145.31	–	Milk samples	[40]
Electrochemiluminescent method	0.01-1.0 (ppb)	0.003 (ppb)	95.2-102.4	5.3-11.2	Dairy products	[41]
Electrochemical detection (3,4-dihydroxyphenylacetic acid as recognition element)	10-5000	3.0	96	–	Milk products	[42]
Electrochemical detection (ascorbic acid as recognition element)	10-350	1.5	98.5-102.5	1.32-2.58	Infant formula and milk samples	This work

Table 2. Determination results of MEL in spiked samples (n = 3)

Samples	Added (nM)	Found (nM)	RSD (%)	Recovery (%)
Infant formula				
1	100	102.5	1.32	102.5
2	200	196.9	2.58	98.5
3	300	296.1	1.69	98.7
Milk				
1	100	99.2	2.24	99.2
2	200	198.6	2.31	99.3
3	300	303.5	1.36	101.2

substances possibly existing in the real samples on the oxidation peak current of 0.5 μM AA were investigated. The results suggested that 200-fold concentration of glucose, lactose, fructose, glycerol, Ca^{2+}, Mg^{2+}, K^{+}, Fe^{3+}, SO_4^{2-}, Cl^{-} barely had any influence on the current signal of AA. Additionally, since the senor is based on the hydrogen-bonding interaction deriving from amidogen of MEL combined with AA, we further tested some compounds which contain amidogen. It was found that 100-fold concentration of glycine, histidine, phenylalanine, tyrosine and tryptophan had no important influence on the current signals of AA with deviations below 5%, indicating that hydrogen-bonding between these amino compounds and AA was very weak and their interference for determination of MEL can be ignored. The results obtained from repeatability, stability and interference tests indicated that this technique might be suitable for analytical application.

Determination of MEL in Practical Samples. In order to ascertain the potential applications in practical sample analysis, this newly-proposed method was used to detect MEL in infant formula and milk which were bought from the local supermarket. Firstly, the infant formula and milk were pretreated according to the procedure described above. Because the existing food and milk in the market are free of MEL, the practical samples were spiked with certain amounts of MEL standard solution directly. Finally, a known-amount of sample solution was added into pH 6.0 PBS of 0.1 M, and then analyzed under the optimized conditions. Each sample undergoes three parallel measurements, and the determination results are list in Table 2. Attractively, the RSD is below 3%, suggesting that the electrochemical sensor possesses good reproducibility; and the recoveries were in the range from 98.5% to 102.5%, indicating that this method has good accuracy. Therefore, the developed electrochemical sensor is reliable and effective for the determination of MEL in practical samples.

Conclusion

A novel electrochemical method for sensitive detection of MEL was established by the utilization of AA as the recognition element. Firstly, the HAP/MWCNT film was used to heighten the oxidation peak current of AA. With MEL adding in, this peak current decreased observably due to the existing hydrogen bonding and electrostatic interaction. Hence, the decreasing signal was used to detect MEL conveniently. Finally, the prepared electrochemical sensor exhibited excellent advantages, such as simple fabrication, convenient operation, long-term stability and satisfactory repeatability, and it has great potential application in the determination of MEL in infant formula and milk samples.

Acknowledgments. This work is kindly supported by the supports of the Open Fund Project of Key Laboratory in Hunan Universities (No. 09K099, No. 10K010) and the Youth Backbone Teacher Training Program of Hengyang Normal University (2010).

References

1. Ding, N.; Yan, N.; Ren, C.; Chen, X. *Anal. Chem.* **2010**, *82*, 5897.
2. Liu, F.; Yang, X.; Sun, S. *Analyst* **2011**, *136*, 374.
3. Xie, Y.; Huang, Y.; Wang, W.; Liu, G.; Zhao, R. *Analyst* **2011**, *136*, 2482.
4. Dominguez-Estevez, M.; Constable, A.; Mazzatorta, P.; Renwick, A. G.; Schilter, B. *Regul. Toxicol. Pharm.* **2010**, *57*, 247.
5. Zhu, L.; Gamez, G.; Chen, H. W.; Chingin, K.; Zenobi, R. *Chem. Commun.* **2009**, *5*, 559.
6. Sun, Q.; Shen, Y.; Sun, N.; Zhang, G. J.; Chen, Z.; Fan, J. F.; Jia, L. Q.; Xiao, H. Z.; Li, X. R.; Puschner, B. *Eur. J. Pediatr.* **2010**, *169*, 483.
7. Liu, Y.; Deng, J.; An, L.; Liang, J.; Chen, F.; Wang, H. *Food Chem.* **2011**, *126*, 745.
8. Su, H.; Fan, H.; Ai, S.; Wu, N.; Fan, H.; Bian, P.; Liu, J. *Talanta* **2011**, *85*, 1338.
9. Wu, Z.; Zhao, H.; Xue, Y.; Cao, Q.; Yang, J.; He, Y.; Li, X.; Yuan, Z. *Biosens. Bioelectron.* **2011**, *26*, 2574.
10. Roy, B.; Saha, A.; Nandi, A. K. *Analyst* **2011**, *136*, 67.
11. Chi, H.; Liu, B.; Guan, G.; Zhang, Z.; Han, M. Y. *Analyst* **2010**, *135*, 1070.
12. Liang, X.; Wei, H.; Cui, Z.; Deng, J.; Zhang, Z.; You, X.; Zhang, X. E. *Analyst* **2011**, *136*, 179.
13. Attia, M. S.; Bakir, E.; Abdel-aziz, A. A.; Abdel-mottaleb, M. S. A. *Talanta* **2011**, *84*, 27.
14. Xiang, D.; Zeng, G.; Zhai, K.; Li, L.; He, Z. *Analyst* **2011**, *136*, 2837.
15. Zeng, H. J.; Yang, R.; Wang, Q. W.; Li, J. J.; Qu, L. B. *Food Chem.* **2011**, *127*, 842.
16. Lou, T.; Wang, Y.; Li, J.; Peng, H.; Xiong, H.; Chen, L. *Anal. Bioanal. Chem.* **2011**, *401*, 333.
17. Squadrone, S.; Ferro, G. L.; Marchis, D.; Mauro, C.; Palmegiano, P.; Amato, G.; Poma Genin, E.; Abete, M. C. *Food Control* **2010**, *21*, 714.
18. Sun, H.; Wang, L.; Ai, L.; Liang, S.; Wu, H. *Food Control* **2010**, *21*, 686.
19. Wu, W. C.; Tsai, I. L.; Sun, S. W.; Kuo, C. H. *Food Chem.* **2011**, *128*, 783.
20. Bera, R. K.; Raj, C. R. *Analyst* **2011**, *136*, 1644.
21. Liao, C. W.; Chen, Y. R.; Chang, J. L.; Zen, J. M. *Electroanalysis* **2011**, *23*, 573.
22. Liu, Y. T.; Deng, J.; Xiao, X. L.; Ding, L.; Yuan, Y. L.; Li, H.; Li, X. T.; Yan, X. N.; Wang, L. L. *Electrochim. Acta* **2011**, *56*, 4595.
23. Jin, G. P.; Yu, B.; Yang, S. Z.; Ma, H. H. *Microchim. Acta* **2011**, *174*, 265.
24. Liang, R.; Zhang, R.; Qin, W. *Sens. Actuators B* **2009**, *141*, 544.
25. Zhu, H.; Zhang, S.; Li, M.; Shao, Y.; Zhu, Z. *Chem. Commun.* **2010**, *46*, 2259.
26. Li, J.; Kuang, D.; Feng, Y.; Zhang, F.; Liu, M. *Microchim. Acta* **2011**, *172*, 379.

27. Wang, H.; Zhai, L.; Li, Y.; Shi, T. *Mater. Res. Bull* **2008**, *43*, 1607.
28. Li, L.; Li, B.; Cheng, D.; Mao, L. *Food Chem.* **2010**, *122*, 895.
29. Li, F.; Li, J.; Feng, Y.; Yang, L.; Du, Z. *Sens. Actuators B* **2011**, *157*, 110.
30. Mbouguen, J. C. K.; Kenfack, I. T.; Walcarius, A.; Ngameni, E. *Talanta* **2011**, *85*, 754.
31. Kumar, S. A.; Lo, P. H.; Chen, S. M. *Biosens. Bioelectron.* **2008**, *24*, 518.
32. Laviron, E. *J. Electroanal. Chem.* **1974**, *52*, 355.
33. Zheng, X.; Zhou, D.; Xiang, D.; Huang, W.; Lu, S. *Russ. J. Electrochem.* **2009**, *45*, 1183.
34. Bond, A. M. *Modern Polarographic Methods in Analytical Chemistry*; Marcel Dekker: New York, 1980; pp 236-287.
35. Li, G.; Yang, S.; Qu, L.; Yang, R.; Li, J. *J. Solid State Electrochem.* **2011**, *15*, 161.
36. Motahary, M.; Ghoreishi, S. M.; Behpour, M.; Golestaneh, M. *J. Appl. Electrochem.* **2010**, *40*, 841.
37. Anson, F. *Anal. Chem.* **1964**, *36*, 932.
38. Adams, R. N. *Electrochemistry at Solid Electrodes*; Marcel Dekker: New York, 1969; pp 280-283.
39. Cao, Q.; Zhao, H.; Zeng, L.; Wang, J.; Wang, R.; Qiu, X.; He, Y. *Talanta* **2009**, *80*, 484.
40. Choi, J. H.; Kim, Y. T.; Lee, J. H. *Analyst* **2010**, *135*, 2445.
41. Guo, Z.; Gai, P.; Hao, T.; Wang, S.; Wei, D.; Gan, N. *Talanta* **2011**, *83*, 1736.
42. Cao, Q.; Zhao, H.; He, Y.; Ding, N.; Wang, J. *Anal. Chim. Acta* **2010**, *675*, 24.